Journal of Thermal Science Vol.31, No.3 (2022) 882–894

https://doi.org/10.1007/s11630-022-1473-4 **Article ID: 1003-2169(2022)03-0882-13**

Nonlinear Dynamic Characteristics of Turbulent Non-Premixed Acoustically Perturbed Swirling Flames

ZHOU Hao*, TAO Chengfei, MENG Sheng, CEN Kefa

State Key Laboratory of Clean Energy Utilization, Zhejiang University, Hangzhou 310027, China

Abstract: The main objective of this article was to experimentally investigate the dynamic response of diffusion flame under acoustic excitation in a laboratory-scale burner. Two parametric variations of the burner, the burner inlet length and variation of the airflow rate, were studied. Experimental results were analyzed through nonlinear time series analysis and several resonance characteristics were obtained. Results indicate that the flame-acoustic resonance only appears under certain frequencies together with the fuel tube vibration. Resonance characteristics of the combustion chamber and air inlet in the non-premixed burner indicate quasi-periodic or limit cycle oscillations, respectively. Flame-acoustic resonance would trigger the frequency and amplitude mode-transition in burners. Moreover, the intermittency of flame heat release was observed under variation of inlet length and airflow rate in the burner; the 445 mm case shows more frequency peaks and fluctuations than the 245 mm one. Four typical flame forms were examined during the flame-acoustic resonance conditions, evolves from wrinkled flames to diverged flames, then evolves to reattached flames and finally to blow-off flames. This study proposed the practical application of nonlinear time-series analysis method as a detection tool for flame-acoustic resonance in laboratory non-premixed burners, which could contribute to the detection and prevention of potential thermoacoustic instabilities or resonance structure failures of industrial boilers. Finally, this study demonstrates an alternative to conventional linear tool for the characterization of nonlinear acoustic resonance in industrial boilers.

Keywords: flame-acoustic resonance, non-linear time series analysis, non-premixed burners, intermittency, dynamic characteristics

1. Introduction

In combustion-based propulsion systems, thermo-acoustic instability is an undesired phenomenon which can cause serious pressure fluctuations and serve damages to the combustor components [1, 2]. Thermo-acoustic instability is an inherently nonlinear process and involves many complex factors in industrial burners which makes thermoacoustic modeling sophisticated [3]. Dynamic characteristics of burners with different geometry, emission, pilot burners, and fuel characteristics were widely studied [4–8]. The intermediate nonlinearity and sensitivity of burner contribute to the difficulty of understanding flame-acoustic resonance characteristics and damping of thermoacoustic instabilities [9]. However, the nonlinear time-series analysis tools are mainly used

Received: Oct 08, 2019 AE: YANG Bin Corresponding author: ZHOU Hao E-mail: zhouhao@zju.edu.cn

Nomenclature

AMI	average mutual information	L_2	air inlet length/mm
CH*	chemiluminence	P_1	section pressure/Pa
D	chamber width/mm	P_2	inlet acoustic pressure/Pa
d_E	embedding dimension	PMT	photomultiplier tube
FEM	Finite Element Method	**Greek symbols**	
FFT	Fast Fourier Transform	τ	optimum time delay/ms
L	chamber length/mm	Φ	equivalence ratio
L_1	air inlet length/mm		

to study the dynamics of premixed combustion [10–27]. Although time-frequency analysis has been applied to the fault detection of diesel engines [28], the dynamic characteristics of non-premixed combustion in industrial non-premixed combustors are not well studied. Mechanism of resonance behind flame-acoustic coupling interaction is seldom explored by nonlinear time series tools.

Combustion instability is a serious problem in industrial thermal power plants. One must identify the intermediate dynamic states of the system in order to fully comprehend the system and obtain complete characterization. Larry [10–12] investigated the periodic and aperiodic thermoacoustic oscillations by acoustic forcing. Sujith [13–20] studied combustion instabilities with the nonlinear time series analysis tools by exploring the domain of intermittency, bifurcation and blowout characteristics during thermoacoustic oscillations. Kabiraj [21] studied recurrence quantification to analyze the combustion noise and revealed that thermoacoustic instability exhibits several different dynamic states. Juniper [22] identified the bifurcations and chaos in self-excited thermoacoustic oscillations by phase portraits and Poincaré sections. With the concept of dynamical system theory, Gotoda [23–25] found that the combustion blowout can be detected and prevented through nonlinear time-series analysis. Unlike premixed flames, non-premixed flames can be hydro-dynamically unstable and oscillate at a low natural frequency [26]. Although nonlinear time-series analysis techniques were widely used to study thermoacoustic instabilities in premixed combustors [27–29], the resonance characteristics of non-premixed burners under acoustic excitations are not well studied. Through changing the flame position and airflow rate, Sen [30–31] obtained several interesting dynamic characteristics in self-excited inverse diffusion flames with recurrence analysis, such as limit cycles, intermittency, and homoclinic orbits. Guan [32] studied dynamic characteristics of high-frequency thermoacoustic oscillations in a solid rocket motor with nonlinear time-series analysis and observed transient mode switching between different unstable attractors. Kim [33] examined nonlinear mode transition mechanisms of a self-excited Jet A-1 spray non-premixed flame with nonlinear time-series analysis tools. Zhou [34] explored dynamic characteristics of non-premixed swirl-stabilized flames to acoustic excitation through Poincaré Sections analysis and concluded that lock-in occurred more easily when the forcing frequency was greater than the natural frequency. The recent research [35] identified that burner geometry also affects non-premixed flame response under acoustic excitation, but the specific physical mechanism behind this nonlinear resonance phenomenon is still unknown. Further research with nonlinear analysis tools is needed.

The purpose of the present work is to explore the flame-acoustic resonance characteristics of a laboratory-scale non-premixed burner under acoustic disturbance with nonlinear dynamical system theory. With the nonlinear time series analysis tools [36–38] and COMSOL acoustic simulation techniques [39–42], the effects of burner inlet length and airflow rate on the non-premixed flame-acoustic resonance characteristics were investigated. Under flame-acoustic resonance conditions, the sound pressure fluctuation, heat release intermittency and flame morphology phenomena of the non-premixed burner were studied simultaneously. The resonance characteristics detection of a non-premixed burner through nonlinear time series analysis has not been studied before, therefore this study can lead to a better understanding of flame-acoustic resonance dynamic characteristics. As a result, providing a useful tool for detecting unsteady resonance characteristics among non-premixed burners can improve the operation safety of industrial boilers.

2. Experimental Setup and Analytical Methods

Experiments were performed on a laboratory-scale, swirl-stabilized non-premixed burner. Detailed experimental setup and indispensable instruments used in the present work are shown in Fig. 1 as a system diagram and the components of the experiment are connected in series by black lines. Combined with two symmetrically

installed loudspeakers, the overall layout and measuring instruments of the burner are demonstrated in Fig. 2(a). The non-premixed flame was perturbed acoustically by the above loudspeakers, accompanied by amplified figures of the combustion chamber illustrated in Fig. 2(b) and swirlers in Fig. 2(c). It is presented in Fig. 1 and Fig. 2 that at the upstream of the burner, the geometry structure of the burner inlet channel comprises a cylindrical air inlet section and a fuel tube. An optically-accessible combustion chamber with three quartz square windows is arranged in the middle of the burner. The quartz windows were rubbed by ethyl alcohol before experiments for a better transmittance. Fig. 2(c) and (d) show the swirler of the burner. The axial and azimuthal velocities of the burner are assumed to be uniform and the vanes are very thin [3]. The diameter of

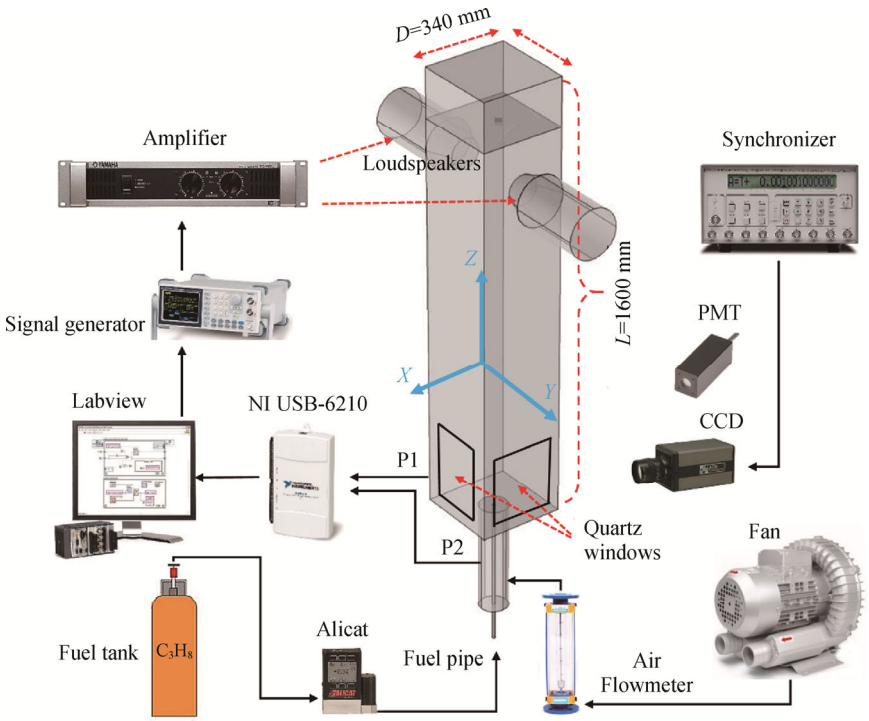

Fig. 1 System diagram of the acoustically perturbed non-premixed swirling burner (P1, P2: Position of sound pressure tap)

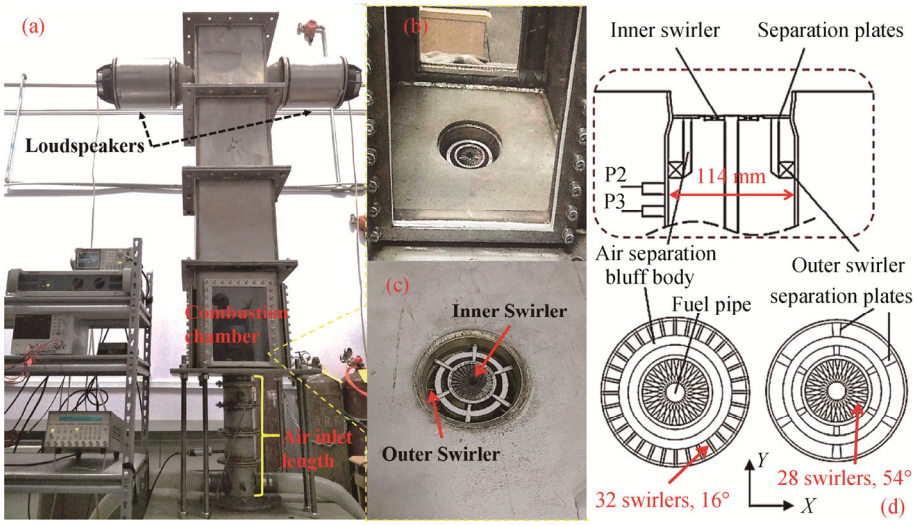

Fig. 2 (a) The layout of the non-premixed combustor with 445 mm and 225 mm air inlet length; (b) Magnified figure of the combustion chamber; (c) Magnified figure of swirlers; (d) The detailed configuration of the burner with separation plates, inner and outer swirlers (P2, P3: Position of sound pressure tap)

the burner inlet section is 114 mm. Inner swirler has 28 swirl vanes with thickness of 0.5 mm, aligned at 54° to the flow direction. Outer swirler has 32 swirl vanes with thickness of 1 mm and 16° angle.

The cross-sectional area of the combustor chamber is 340 mm×340 mm, labeled in Fig. 1. Settings of the air inlet length elected with two different values, L_1=245 mm and L_2=445 mm. The length of the combustion chamber and exhaust section is fixed at L=1600 mm; the width of the combustion chamber is D=340 mm, while two loudspeakers (150 W each, HiVi, D10G) locates at the 1400 mm downstream of the combustor and connects to a power amplifier (Yamaha, P5000S) through two audio signal wires (Zoguo, 3.2 mm×6.4 mm). The input voltage level of two loudspeakers keeps the same during excitation experiments. The burner is excited by the signal generator with the frequency of 30–400 Hz. The sweeping frequency gradient is set to 10 Hz during the period of 30–400 Hz, and 1 Hz for the flame-acoustic resonance region.

Sound pressure of the combustion chamber is gathered through a pressure transducer; the pressure transducers are installed at the wall of the chamber [34]. Flame heat release signal is measured with a photomultiplier tube; the sound pressure and CH* chemiluminescence signal is recorded simultaneously using a multi-channel signal recorder with a 20 kHz sampling rate [35]. The experimental data are transmitted and processed by using Labview2012 and Matlab2017a commercial software. In Fig. 1, along with the PMT (photomultiplier tube), the non-premixed flame images during the resonance process are recorded synchronously using a high-speed camera. The sweep frequency of the loudspeaker is controlled by the arbitrary signal generator; the amplitude of the sound excitation is kept constant during the experiments [34, 35].

Air for combustion is conveyed through two radially opposed apertures at the upstream of the burner. In the present work, the combustor is operated at atmospheric pressure and ambient temperature. Propane is delivered through the central stainless fuel pipe to the combustion chamber in this study. The inner diameter of the fuel tube is 13 mm. In Fig. 1, volume flow rate of the fuel is adjusted with two mass flowmeters and the thermal power of the combustor is fixed, with the propane flow rate fixed at 9.6 L/min. The propane is provided with fuel tanks. The air is supplied with an industrial fan and the flow rate is controlled by a volumetric flowmeter. During the combustion, the global equivalence ratio of 0.3 and 0.18 are selected. Combustion conditions of the flame-acoustic resonance process explored are summarized in Table 1.

Commercial FEM software, COMSOL Multiphysics [39], has been taken to investigate the acoustic mode of non-premixed burners with different inlet lengths. COMSOL Multiphysics has been combined with nonlinear polynomial flame response models to study the thermoacoustic oscillations in the simple laboratory-scale longitudinal combustor and an annular combustion chamber [40, 41]. In COMSOL acoustic modules, linearized potential flow equation, linearized-Euler equation or linearized equation can be solved. The Navier-Stokes equations are used to study the aeroacoustics [42]. Before acoustic FEM computation of the burner, working fluid medium of the non-premixed burners was regarded as ideal gases; the speed of sound in air was set as 343 m/s; density of air was set as 1.2 kg/m^3; air temperature in the inlet section was defined as 25°C; air temperature in the combustion chamber was defined as 1270°C. Nonlinear time series analysis methods contain phase space reconstruction and poincaré section, optimal time delay τ and embedding dimension d_E, recurrence qualification analysis [29–38].

Table 1 Combustion conditions of acoustically perturbed non-premixed flame studied in the experiment

Air inlet length/ mm	Chamber length/ mm	C_3H_8 flow rate/ L·min^{-1}	Airflow rate/ L·min^{-1}	Global Φ –	Forcing frequencies/ Hz
245	1600	9.6	760/1270	0.30/0.18	30–400
445	1600	9.6	760/1270	0.30/0.18	30–400

3. Results and Discussion

3.1 Sound pressure resonance characteristics analysis

To find the given frequency that flame-acoustic resonance occurs in the burner, the nonlinear dynamic characteristics of non-premixed flames under acoustic excitation were studied in our previous research [35]. The peak pressure response of flame in the combustion chamber is recorded.

To further elucidate the flame-acoustic resonance characteristics, the acoustic resonance of the burner was explored by FEM (Finite Element Method) in COMSOL software [39]. Fig. 3 and Fig. 4 present the results of acoustic simulation of the burner with COMSOL software. For Case L_1=245 mm, air inlet and fuel tube of the non-premixed burner resonate simultaneously at 60 Hz; the maximum vibration emerges in the fuel tube; P is the non-diamensional value of the sound pressure by FEM. At 144 Hz, the combustion chamber and air inlet no longer resonate with the fuel tube, but the maximum sound pressure emerges in the fuel tube. At the response frequency of 190 Hz, the fuel tube of the burner no longer resonates, but the maximum vibration emerges in

the air inlet. In Fig. 4, the resonance characteristics of L_2=445 mm length resemble that present in Case L_1=245 mm. The numerical results presented in Fig. 3 and Fig. 4 are conformed to the experimental results presented in Ref. [35]. Under conditions of flame-acoustic resonating (L_1: 144 Hz, L_2: 134 Hz), the vibrating fuel pipe causes the fluctuation of heat release rate.

We could draw from the COMOSOL simulation results in Fig. 3 and Fig. 4 that the resonance modes in both 445 mm and 245 mm cases are mixed resonance mode of the fuel pipe, combustion chamber and air inlet section. The dynamic characteristics of non-premixed flame under acoustic resonance will be studied in the next section.

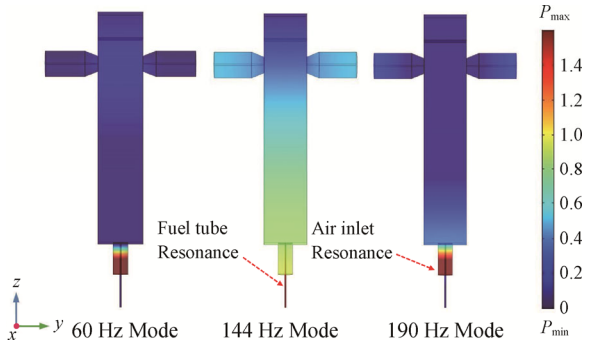

Fig. 3 FEM acoustic simulation of the burner with 245 mm inlet length compared with the results in Ref. [35]

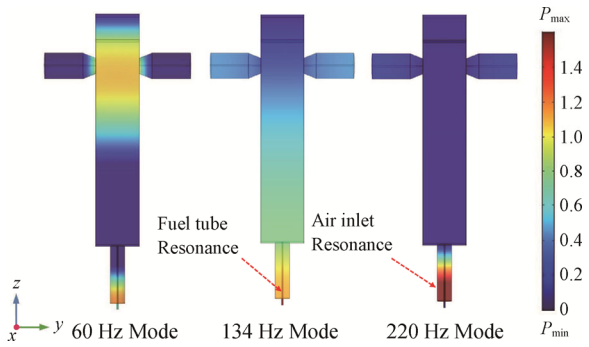

Fig. 4 FEM acoustic simulation of the burner with 445 mm inlet length compared with the results in Ref. [35]

In order to study the dynamic characteristics of sound pressure and flame in the case of resonance, the nonlinear time series analysis method is used [29–38]. Eight different conditions of experiments were designed through calculating the minimum delay time τ and embedding dimension d_E of time series in the combustion chamber and burner inlet parts. The AMI (average mutual information) approaches minimum when time delay τ=0.5. The embedding dimension used for nonlinear dynamics research is d_E=10. With the above optimum delay time τ and embedding dimension d_E, the time series of pressure in the combustion chamber and burner inlet sections are analyzed sequentially with phase space reconstruction, poincaré sections, and recurrence qualification analysis. The sampling frequency was set as 2000 HZ; the time series of pressure was set as 0.2 s for analyzing. The phase space figure of Fig. 5(a) and Fig. 5(b) denotes that the sound pressure in combustion chamber is in chaotic states at Φ=0.18 and evolves to quasi-periodic states at Φ=0.30. This is compatible with the acoustic simulation results demonstrated in Fig. 4, which suggests that the resonance states in the combustion chamber are complex and in conformity. The poincaré section graph in Fig. 5 and Fig. 6 shows a scattered distribution, which means that the dynamic characteristics of sound pressure in the combustion chamber are in combustion noise states at Φ=0.18 and evolves to periodic limit cycle states at Φ=0.30. It can be seen that in Fig. 5(b), Fig. 6(a) and Fig. 6(b), the recurrence qualification of the periodic oscillating system appears along the main diagonal with equal intervals. This diagram indicates chaotic states of the sound pressure combustion chamber. Fig. 5(a-1) shows the phase space reconstruction of sound pressure. The phase space diagrams were composed of chaotic points. Fig. 5(a-2) shows the poincaré sections of phase space. The points are sparsely distributed near the diagonal line. As seen in Fig. 5(a-3), the recurrence qualification graph is composed of a large number of isolated points and some short diagonals, showing a chaotic structure with inherent certainty. This structure indicates quasi-periodic states of the combustion chamber.

Accordingly, by analyzing the dynamic characteristics of the sound pressure of the burner inlet section presented in Fig. 7 and Fig. 8, it can be seen that the burner inlet section is in a periodic limit cycle oscillation states under acoustic resonance, which is different from results shown in Fig. 5 or Fig. 6. The computational domain in Fig. 7 and Fig. 8 was set as 0.2 s with 400 sampling points. Compared with the acoustic simulation results in Fig. 3 and Fig. 4, under flame-acoustic resonating (144 Hz, 134 Hz), the combustion chamber and air inlet of the burner show different strengths of resonance, which matches the dynamic characteristics of the combustion chamber and air inlet presets in Figs. 5–8.

The phase space figures of Fig. 7 and Fig. 8 denote that the sound pressure in the combustion chamber is in the turbulent limit cycle states at Φ=0.18 and Φ=0.30. This is consistent with the acoustic simulation results demonstrated in Fig. 4, which indicates intense periodic resonance states in the air inlet section. The poincaré section graphs in Fig. 7 and Fig. 8 are in compacted distribution, which means that the dynamic characteristics of sound pressure in air inlet are in a stable limit-cycle states at Φ=0.18 and Φ=0.30. It can be

seen that in Fig. 7 and Fig. 8, the recurrence qualification of the sound pressure in air inlet appears along the main diagonal with equal intervals. This structure indicates that under flame-acoustic resonance, the sound pressure in the air inlet shows periodic states.

3.2 Flame resonance characteristics analysis

Fig. 9 and Fig. 10 present the recurrence qualification analysis of PMT (photomultiplier tube) signal under flame-acoustic resonance, with different equivalence ratios and inlet lengths. There are sudden fluctuations of flame heat release under acoustic-flame resonance. Dynamic characteristics of higher equivalence ratio in both cases lead to higher flame heat release fluctuation. The fluctuation phenomena in Fig. 9 and Fig. 10 conforms to the COMSOL acoustic simulation results of the fuel inlet pipes oscillation modes presented in Fig. 3 and Fig. 4. The sound pressure fluctuation in the 245 mm case is more intense than the 445 mm case. However, this is poles apart when referring to the heat release

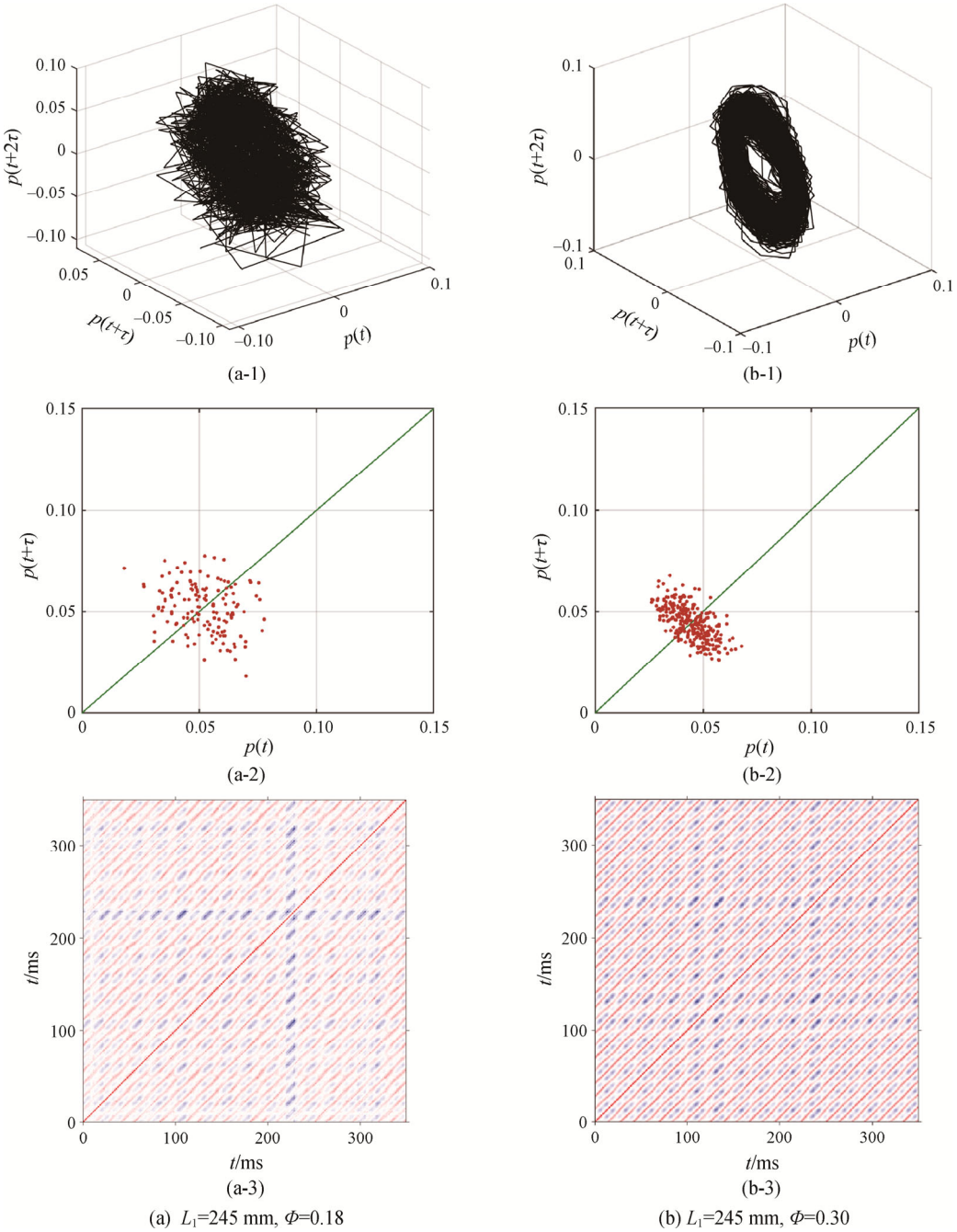

(a) L_1=245 mm, Φ=0.18 (b) L_1=245 mm, Φ=0.30

Fig. 5 Nonlinear time-series analysis for combustion section with inlet length of 245 mm and different equivalence ratio (Φ =0.18 or 0.30) ($p(t+2\tau)$, $p(t+\tau)$ and $p(t)$ denote the time-series of sound pressure.)

fluctuation in the 245 mm case compared with the 445 mm case.

Nonlinear dynamic characteristics of flame heat release rate are different from sound pressure in the combustion chamber. In Fig. 11, FFT analysis shows the 445 mm case exhibits higher heat release intensity than the 245 mm case. Furthermore, the heat release intensity gradually declines as the oscillation frequency increases. A relatively stable level with some sudden oscillations was maintained in the end. The sampling frequency was 2000 Hz; the time series of heat release rate was set as 2 s (with 4000 sampling points) for analyzing. Fig. 12 shows the time-series signal of flame heat release rates. More fluctuations emerge under the condition of 445 mm inlet lengths. These results conform to the experimental results presented in Fig. 9 and Fig. 10.

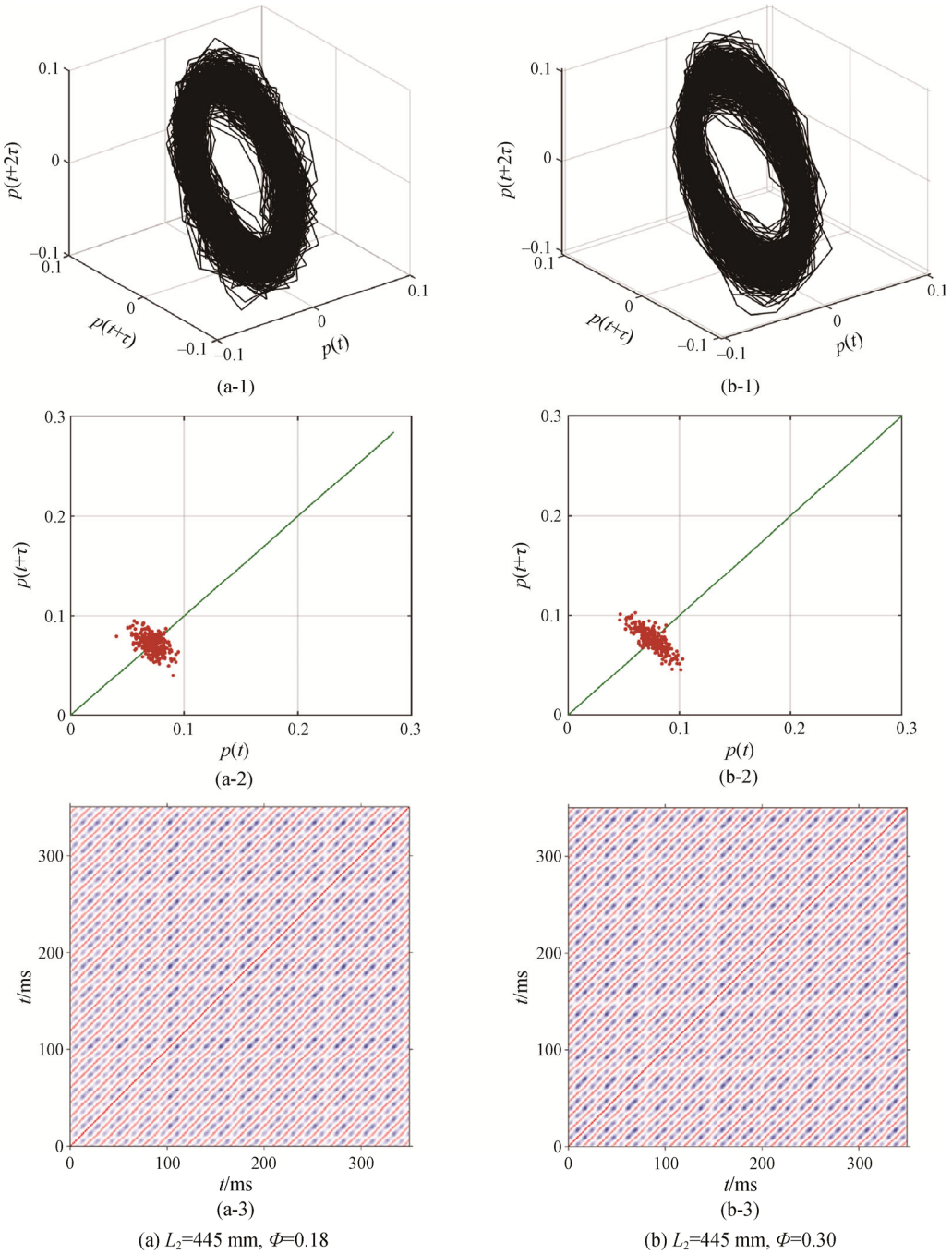

Fig. 6 Nonlinear time-series analysis for combustion section with inlet length of 445 mm and different equivalence ratio (Φ =0.18 or 0.30)

Flame intermittency was observed and accompanied by four kinds of forms during the mode transition. Images of flame were captured with the high-speed CCD camera under conditions of flame-acoustic resonance. The flame images under flame-acoustic resonance are captured using a digital high-speed camera (AOS S-PRI plus, 800×600 pixels image resolution, 14 μm pixel size) with a sampling rate of 1250 fps. For resonance frequency between 130 Hz (7.7 ms) and 150 Hz (6.7 ms), 10 pictures are used to get the average flame height in the article. As shown in Fig. 13, there are mainly four forms of unstable non-premixed flame, which are the results of the flame-acoustic resonance. The unexcited stable flame is set as Mode-A flame; the original height of the flame is near 300 mm. In the initial resonating stage, the sound field wrinkles the flame surface and fines the flame root

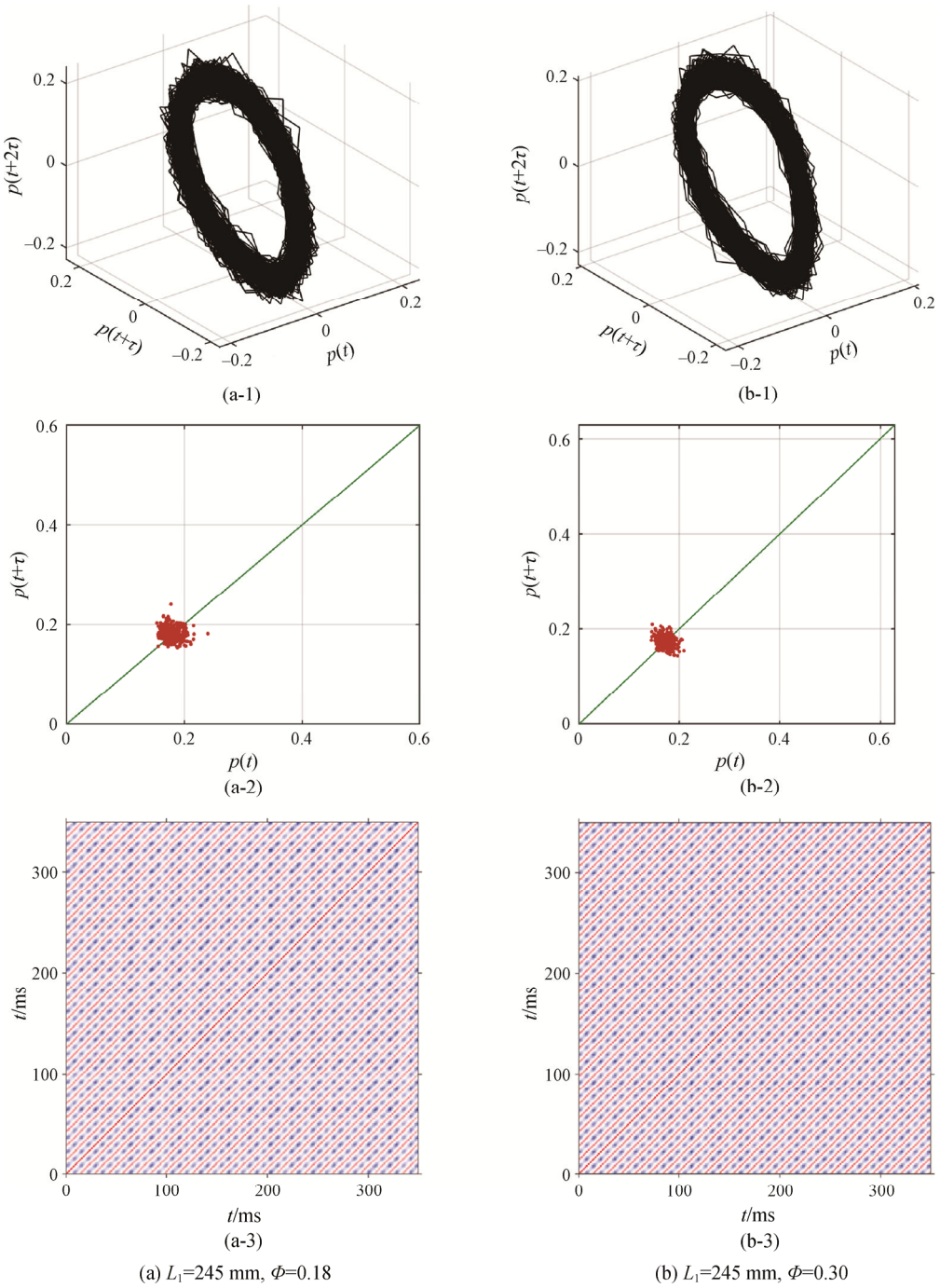

Fig. 7 Nonlinear time-series analysis for inlet air section with inlet length of 245 mm and different equivalence ratio (Φ=0.18 or 0.30)

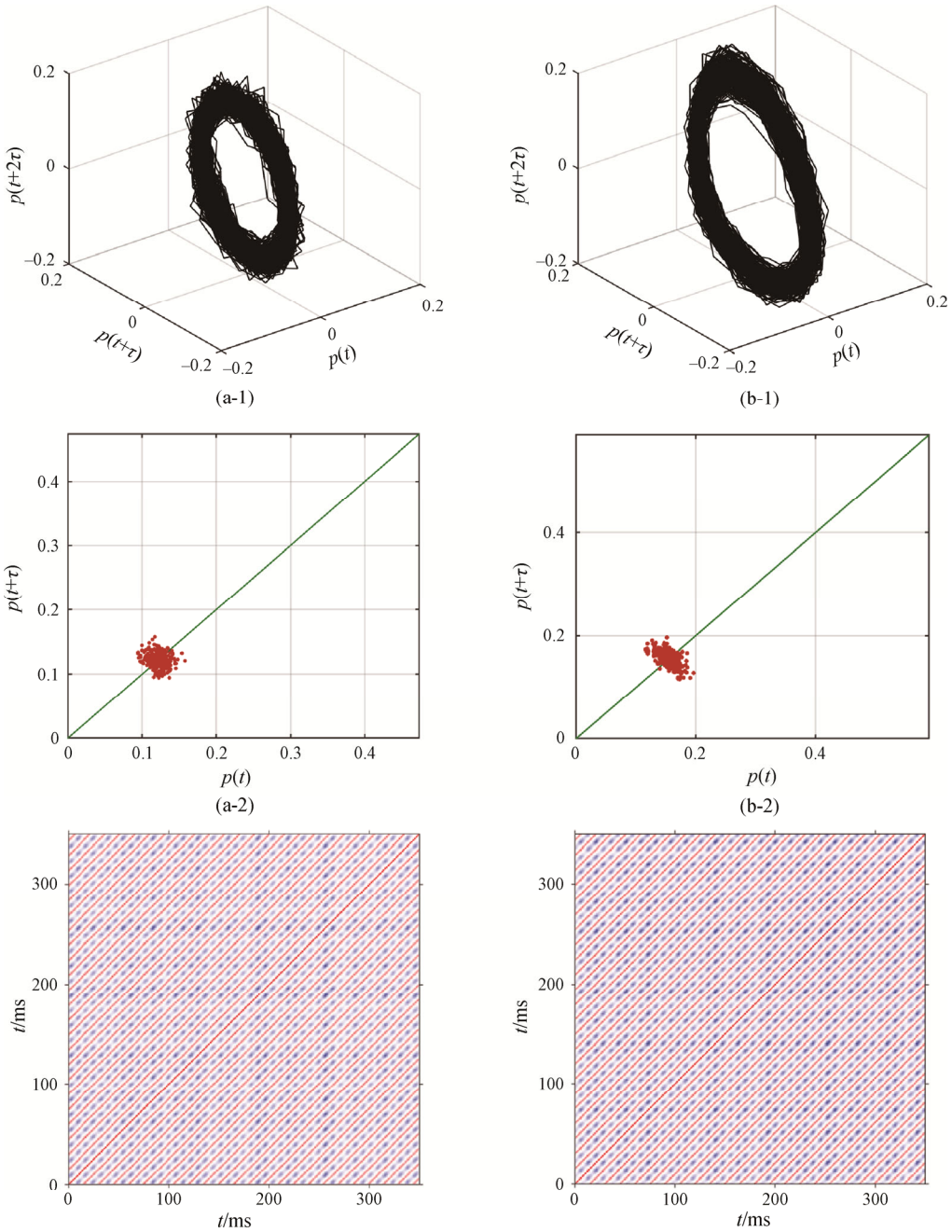

(a) L_2=445 mm, Φ=0.18 (b) L_2=445 mm, Φ=0.30

Fig. 8 Nonlinear time-series analysis for inlet air section with inlet length of 445 mm and different equivalence ratio (Φ =0.18 or 0.30)

(Mode B-Wrinkled flame). Then the flame is strongly coupled with the sound field, resulting in obvious faults and upward movement of the flame (Mode C-Diverged flame); the flame is stretched and becomes slimmer; the average height of the diverged based flame is close to 350 mm. Then the flame stretches severely, rises upward as a whole; the root of the flame disappears, and the flame breaks into several segments (Mode D-Transitional flame). The average height of the transitional reattached flame is close to 200 mm, and then flames become dimmer. Finally, the flame enters a strong turbulent regime and is on the verge of extinction; the flame becomes wider and shorter (Mode E-Lifted-off flame), and the average height of the lifted-off flame is near 100 mm. Rong Fung Huang [43–45] researched non-premixed flames subject to acoustic excitation at resonance conditions, and three different flame modes were observed.

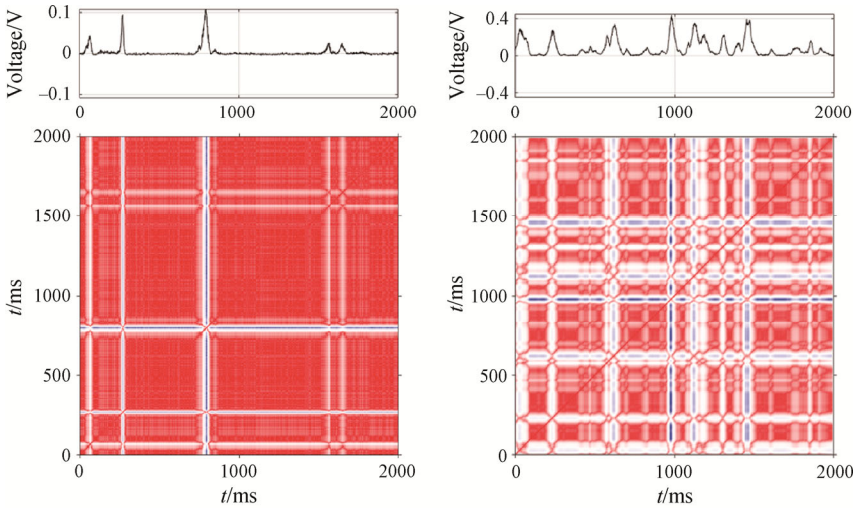

Fig. 9 Recurrence plots of flame heat release fluctuation with inlet length of 245 mm with an equivalence ratio of 0.18 and 0.30 respectively

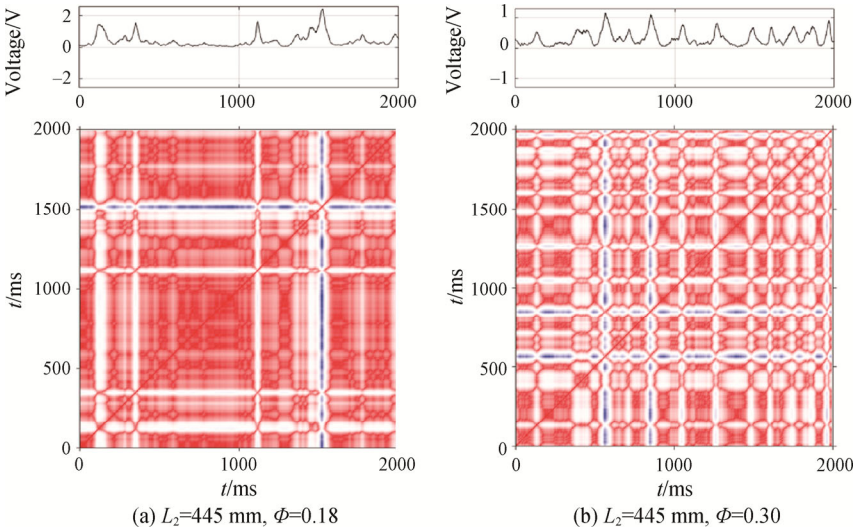

Fig. 10 Recurrence plots of flame heat release fluctuation with inlet length of 445 mm with an equivalence ratio of 0.18 and 0.30 respectively

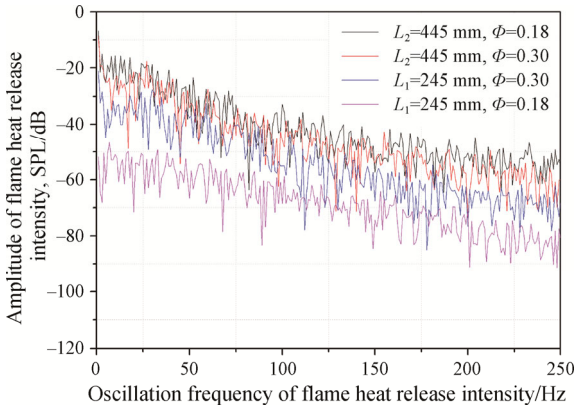

Fig. 11 FFT analysis for flame heat release intensity with inlet length of 245 mm and 445 mm and different equivalence ratio (Φ=0.18 or 0.30)

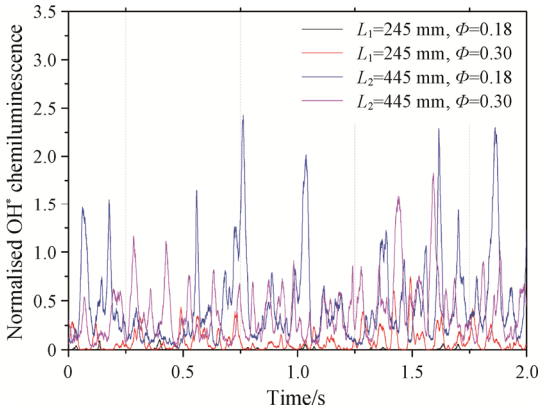

Fig. 12 Time-series of OH^* chemiluminescence for flame heat release rate with inlet length of 245 mm and 445 mm of different equivalence ratio (Φ=0.18 or 0.30)

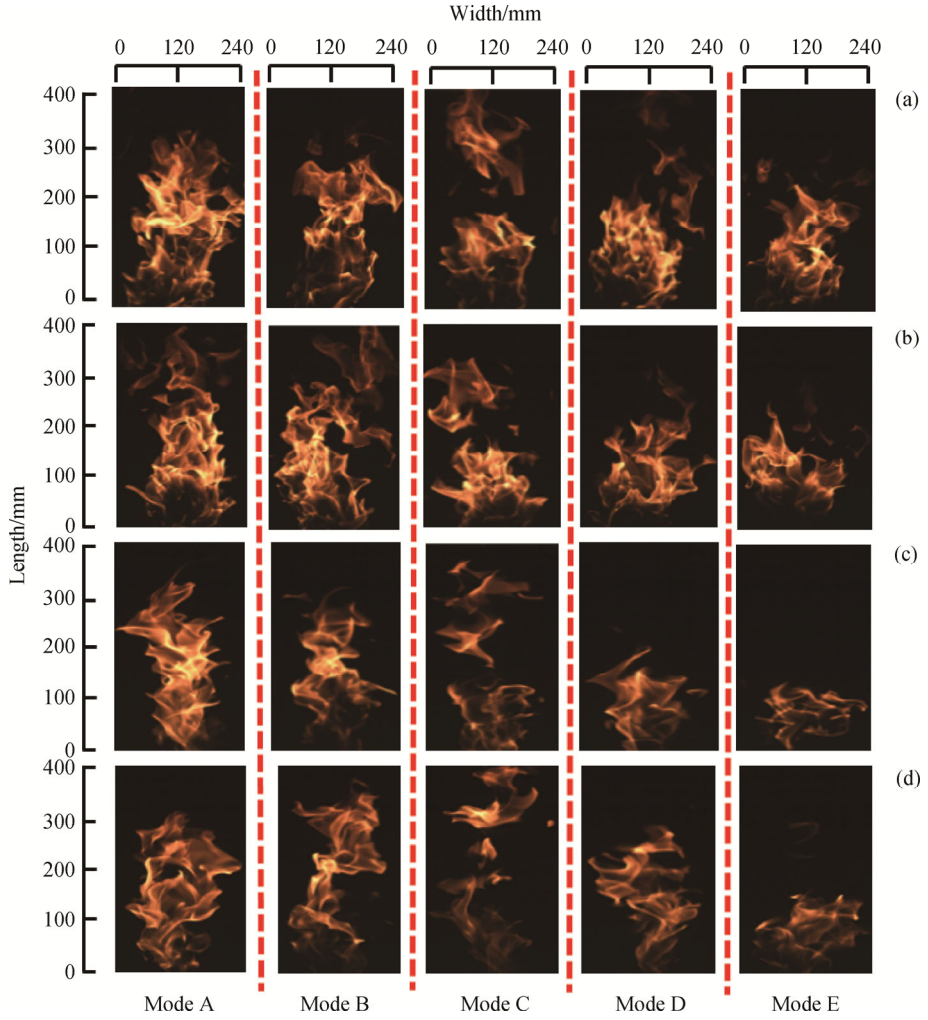

Fig. 13 Far field flame behaviors during resonance: with inlet length of 245 mm and 445 mm at different equivalence ratio. (a) L_1=225 mm, Φ=0.18, 144 Hz. (b) L_1=225 mm, Φ=0.30, 144 Hz. (c) L_1=445 mm, Φ=0.18, 134 Hz. (d) L_1=445 mm, Φ=0.30, 134 Hz.

4. Conclusions

The present work applies time series analysis to explore the nonlinear dynamics of non-premixed flame under flame-acoustic resonance. Two parametric variations of the burner, variation of the burner inlet length and combustion equivalence ratio, were performed. Several dynamic characteristics were revealed. This research provides a tool to study dynamic characteristics of non-premixed flame under resonance and may be of functional significance to the prevention of thermoacoustic instability and resonance structural failure of industrial boilers. Under the flame-acoustic resonance mode, the pressure fluctuation is in chaotic or quasi-periodic states of the combustor chamber, while the pressure fluctuation in the burner air inlet section is in turbulent limit cycle states. Sound pressure in the combustion chamber and air inlet shows frequency-mode-transition phenomena. The frequency and amplitude of the flame-acoustic vary when the inlet length changes. From time-series of the flame heat release rate recorded by PMT, non-premixed acoustically perturbed swirling flame exhibits intense pulsations under flame-acoustic resonance mode. Fuel equivalence ratio and burner inlet lengths have a great influence on flame nonlinear dynamics. During the transition stage, the non-premixed flame has five main forms under the resonance process. The proposed nonlinear time series analysis methods promote a better understanding of resonance dynamics observed in non-premixed combustion burners.

Acknowledgment

This work was supported by National Science Fund for Distinguished Young Scholars (51825605).

References

[1] Lieuwen T., Yang V., Combustion instabilities in gas turbine engines: Operational experience, fundamental mechanisms, and modeling. Progress in Astronautics and Aeronautics, 2005, AIAA, Inc. USA.

[2] Lieuwen T., Unsteady combustor physics. 2012, UK, Cambridge University Press, Cambridge.

[3] Huang Y., Yang V., Dynamics and stability of lean-premixed swirl-stabilized combustion. Progress in Energy and Combustion Science, 2009, 35: 293–364.

[4] Wang X., Lin Y., Zhang C., et al., Effect of swirl cup's secondary swirler on flow field and ignition performance. Journal of Thermal Science, 2015, 24: 488–495.

[5] Xing S., Fang A., Song Q., et al., Experimental investigation of dynamic and emission characteristics of a DLE gas turbine combustor. Journal of Thermal Science, 2013, 22: 180–185.

[6] Jacqueline O., Vishal A., Timothy L., Transverse combustion instabilities: Acoustic, fluid mechanic, and flame processes. Progress in Energy and Combustion Science, 2015, 49: 1–39.

[7] Lin J., Shi Z., Lai H., Numerical study of controlling jet flow and noise using pores on nozzle inner wall. Journal of Thermal Science, 2018, 27: 146–156.

[8] Zhao D., Ephraim G., Philip D., A review of cavity-based trapped vortex, ultra-compact, high-g, inter-turbine combustors. Progress in Energy and Combustion Science, 2018, 66: 42–82.

[9] Juniper M., Sujith R., Sensitivity and nonlinearity of thermoacoustic oscillations. Annual Review of Fluid Mechanics, 2018, 50: 661–689.

[10] Saravanan B., Larry K., Han. Z., et al., Nonlinear dynamics of a self-excited thermoacoustic system subjected to acoustic forcing. Proceedings of the Combustion Institute, 2015, 35: 3229–3236.

[11] Kashinath K., Larry K., Juniper M., Forced synchronization of periodic and aperiodic thermoacoustic oscillations: lock-in, bifurcations and open-loop control. Journal of Fluid Mechanics, 2018, 838: 690–714.

[12] Guan Y., He W., Murugesan M., et al., Control of self-excited thermoacoustic oscillations using transient forcing, hysteresis and mode switching. Combustion and Flame, 2019, 202: 262–275.

[13] Jegadeesan V., Sujith R., Experimental investigation of noise induced triggering in thermoacoustic systems. Proceedings of the Combustion Institute, 2013, 34: 3175–3183.

[14] Vishnu R., Sujith R., Aghalayam P., Role of flame dynamics on the bifurcation characteristics of a ducted V-flame. Combustion Science and Technology, 2015, 187: 894–905.

[15] Nair V., Sujith R., Intermittency as a transition state in combustor dynamics: An explanation for flame dynamics nearing lean blowout. Combustion Science and Technology, 2015, 187: 1821–1835.

[16] Lipika K., Sujith R., Nonlinear self-excited thermoacoustic oscillations: intermittency and flame blowout. Journal of Fluid Mechanics, 2012, 713: 376–397.

[17] Kabiraj L., Saurabh A., Wahi P., et al., Route to chaos for combustion instability in ducted laminar premixed flames. Chaos: An Interdisciplinary Journal of Nonlinear Science, 2012, 22: 023129.

[18] Nair V., Sujith R., A reduced-order model for the onset of combustion instability: physical mechanisms for intermittency and precursors. Proceedings of the Combustion Institute, 2015, 35: 3193–3200.

[19] Unni V., Sujith R., Flame dynamics during intermittency in a turbulent combustor. Proceedings of the Combustion Institute, 2017, 36: 3791–3798.

[20] Nair V., Sujith R., Identifying homoclinic orbits in the dynamics of intermittent signals through recurrence quantification. Chaos: An Interdisciplinary Journal of Nonlinear Science, 2013, 23(3): 033136.

[21] Kabiraj L., Saurabh A., Nawroth H., et al., Recurrence analysis of combustion noise. AIAA Journal, 2015, 53: 1199–1210.

[22] Karthik K., Waugh I., Juniper M., Nonlinear self-excited thermoacoustic oscillations of a ducted premixed flame: bifurcations and routes to chaos. Journal of Fluid Mechanics, 2014, 761: 399–430.

[23] Gotoda H., Nikimoto H., Miyano T., et al., Dynamic properties of combustion instability in a lean premixed gas-turbine combustor. Chaos, 2011, 21: 013124.

[24] Domen S., Gotoda H., Kuriyama T., et al., Detection and prevention of blowout in a lean premixed gas-turbine model combustor using the concept of dynamical system theory. Proceedings of the Combustion Institute, 2015, 35: 3245–3253.

[25] Kobayashi H., Gotoda H., Tachibana S., et al., Detection of frequency-mode-shift during thermoacoustic combustion oscillations in a staged aircraft engine model combustor. Journal of Applied Physics, 2017, 122: 224904.

[26] Li L., Juniper M., Lock-in and quasiperiodicity in hydrodynamically self-excited flames: Experiments and modelling. Proceedings of the Combustion Institute, 2013, 34: 947–954.

[27] Li Ping., Yang E., Song S., et al., Analysis of the dynamic characteristics of combustion instabilities in a pre-mixed lean-burn natural gas engine. Applied Energy, 2016, 183: 746–759.

[28] Taghizadeh A., Mahdavian A., Fault detection of injectors in diesel engines using vibration time-frequency analysis.

Applied Acoustics, 2019, 143: 48–58.

[29] Wu G., Lu Z., Guan Y., et al., Characterizing nonlinear interaction between a premixed swirling flame and acoustics: heat-driven acoustic mode switching and triggering. Energy, 2018, 158: 546–554.

[30] Mondal S., Mukhopadhyay A., Sen S., Dynamic characterization of a laboratory-scale pulse combustor. Combustion Science and Technology, 2014, 186: 139–152.

[31] Sen U., Gangopadhyay T., Bhattacharya C., et al., Dynamic characterization of a ducted inverse diffusion flame using recurrence analysis. Combustion Science and Technology, 2018, 190: 32–56.

[32] Guan Y., Liu P., Jin B., et al., Nonlinear time-series analysis of thermoacoustic oscillations in a solid rocket motor. Experimental Thermal and Fluid Science, 2018, 98: 217–226.

[33] Ahn B., Lee J., Jung S., et al., Nonlinear mode transition mechanisms of a self-excited Jet A-1 spray flame. Combustion and Flame, 2019, 203: 170–179.

[34] Zhou H., Huang Y., Meng S., Response of non-premixed swirl-stabilized flames to acoustic excitation and jet in cross-flow perturbations. Experimental Thermal and Fluid Science, 2017, 82: 124–135.

[35] Zhou H., Meng S., Tao C., et al., Study of burner geometry effects on non-premixed flame response under acoustic excitation. Journal of Low Frequency Noise, Vibration and Active Control, 2019, 38: 3–17.

[36] Kantz H., Schreiber T., Nonlinear time series analysis. Cambridge University Press, 2003, Cambridge, UK.

[37] Marwan N., Romano M., Thiel M., et al., Recurrence plots for the analysis of complex systems. Physics Reports, 2007, 438: 237–329.

[38] Zou Y., Donner R., Norbert M., et al., Complex network approaches to nonlinear time series analysis. Physics Reports, 2019, 787: 1–97.

[39] COMSOL Multiphysics. Acoustic Module Minicourse, 2020.

[40] Oh S., Shin Y., Kim Y., Stabilization effects of perforated plates on the combustion instability in a lean premixed combustor. Applied Thermal Engineering, 2016, 107: 508–515.

[41] Laera D., Campa G., Camporeale S., A finite element method for a weakly nonlinear dynamic analysis and bifurcation tracking of thermo-acoustic instability in longitudinal and annular combustors. Applied Energy, 2017, 187: 216–227.

[42] Kim S., Kim D., Cha D., Finite element analysis of self-excited instabilities in a lean premixed gas turbine combustor. International Journal of Heat and Mass Transfer, 2018, 120: 350–360.

[43] Zargar O., Huang R., Hsu C., Flames of swirling double-concentric jets subject to acoustic excitation at resonance. Journal of Thermal Science and Engineering Applications, 2019, 11(3): 031004.

[44] Zargar O., Huang R., Hsu C., Effect of acoustic excitation on flames of swirling dual-disk double-concentric jets. Experimental Thermal and Fluid Science, 2019, 100: 337–348.

[45] Loretero M., Huang R., Effects of acoustic excitation on a swirling diffusion flame. Journal of Engineering for Gas Turbines and Power, 2010, 132: 1113–1122.